

# Global analysis of color fluctuation effects in proton– and deuteron–nucleus collisions at RHIC and the LHC

M. Alvioli,<sup>1</sup> L. Frankfurt,<sup>2,3</sup> D.V. Perepelitsa,<sup>4</sup> and M. Strikman<sup>3</sup>

<sup>1</sup>*Consiglio Nazionale delle Ricerche, Istituto di Ricerca per la Protezione Idrogeologica, via Madonna Alta 126, I-06128 Perugia, Italy*

<sup>2</sup>*Tel Aviv University, Tel Aviv, Israel*

<sup>3</sup>*104 Davey Lab, The Pennsylvania State University, University Park, PA 16803, USA*

<sup>4</sup>*University of Colorado, Boulder, CO 80309 USA*

(Dated: September 19, 2018)

We test the hypothesis that configurations of a proton with a large- $x$  parton,  $x_p \gtrsim 0.1$ , have a smaller than average transverse size. The application of the QCD  $Q^2$  evolution equations shows that these small configurations also have a significantly smaller interaction strength, which has observable consequences in proton – nucleus collisions. We perform a global analysis of jet production data in proton– and deuteron–nucleus collisions at RHIC and the LHC. Using a model which takes a distribution of interaction strengths into account, we quantitatively extract the  $x_p$ -dependence of the average interaction strength,  $\sigma(x_p)$ , over a wide kinematic range. By comparing the RHIC and LHC results, our analysis finds that the interaction strength for small configurations, while suppressed, grows faster with collision energy than does that for average configurations. We check that this energy dependence is consistent with the results of a method which, given  $\sigma(x_p)$  at one energy, can be used to quantitatively predict that at another. This finding further suggests that at even lower energies, nucleons with a large- $x_p$  parton should interact much more weakly than those in an average configuration, a phenomenon in line with explanations of the EMC effect for large- $x_p$  quarks in nuclei based on color screening.

PACS numbers: 14.20.Dh, 25.40.Ve, 13.85.-t, 25.75.

Hadrons are composite, quantum mechanical systems with a varying spatial and momentum configuration of their internal quark and gluon constituents. In sufficiently high energy processes, these configurations remain approximately fixed during the time of the collision. Thus certain physical properties of the parton system of a rapidly moving hadron, such as the total transverse area occupied by the color fields, may change collision by collision, a phenomenon we refer to as *color fluctuations* [1, 2]. These variations in the internal structure of hadrons have a wide range of observable consequences, such as inelastic diffraction [3–5]. In quantum chromodynamics (QCD), the configurations in which a large ( $> 10\%$ ) fraction of the hadron’s momentum is carried by a single parton are spatially compact. For these cases, in the wide range of energies where non-linear (saturation) effects are expected to be small [6, 7], the interaction strength of the entire configuration decreases along with the overall area occupied by color (for a review and references see Ref. [8]). Furthermore, while the interaction strength for such small configurations is reduced overall, it rises rapidly with collision energy due to a fast increase of the gluon density at small  $x$ . In this paper, we quantitatively investigate these properties of QCD systems in proton– and deuteron–nucleus ( $p/d+A$ ) collision data at the Large Hadron Collider (LHC) and the Relativistic Heavy Ion Collider (RHIC), respectively.

Fig. 1 symbolically illustrates how proton configurations of two different sizes contribute to  $p+A$  interactions. For many processes, a large number of projectile configurations contribute to a studied observable, resulting in a lack of sensitivity to color fluctuation effects. However, in processes to which only a restricted subset of projectile configurations contribute, these effects are important for understanding the experimental data. Historically, they have played a role in interpreting multiplicity distributions in nuclear collisions [9] and in describing the coherent diffractive production of dijets [10–12][13].

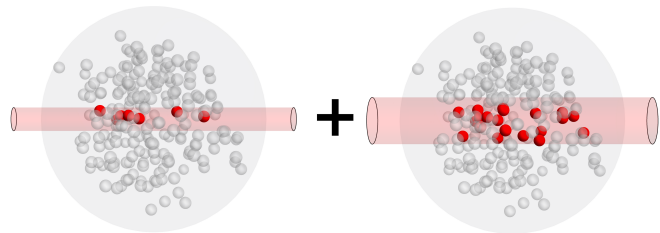


FIG. 1. Schematic representation of a proton–nucleus collision with a fixed geometry of the target nucleus, with a more weakly (more strongly) interacting projectile proton on the left (right). The red tube shows the projection of the projectile proton’s transverse size through the nucleus, with impacted nucleons in red. Typical observables have contributions from both types of events, while large- $x_p$  configurations may preferentially select weakly interacting cases (left).

Experimentally,  $p+A$  collisions with a restricted subset of projectile configurations may be selected with a special trigger such as a hard QCD or electroweak process involving a large- $x_p$  ( $\gtrsim 0.1$ ) parton in the proton [14]. In these large- $x_p$  configurations, color charge screening

within the dominant Feynman diagrams suppresses the gluon field and density of  $q\bar{q}$  pairs, leading to an interaction cross-section which is smaller but grows rapidly with energy (for a review of this phenomenon in HERA data, see Ref. [15]).

The success of the quark counting rules [16, 17] indicates what chain diagrams dominate at large  $x$ . Analysis of these Feynman diagrams [18] indicates that quark transverse momenta should be rather large and hence the 3q configurations should have size much smaller than average. [19].

In  $p+A$  collisions, the shrinking of the proton configuration in large- $x_p$  scattering events should lead to a decrease in the average number of nucleon–nucleon ( $NN$ ) interactions between the projectile and target nucleus,  $\nu$ , relative to that for collisions with a more typical proton configuration. In the  $p+A$  case,  $\nu$  also coincides with the number of wounded nucleons in the target nucleus. This feature should also be present in  $d+A$  collisions, although the magnitude of the effect is diminished due to the unaffected nucleon in the deuteron contributing with an average over its configurations.  $\nu$  is indirectly measured in experiments via the soft particle multiplicity [20–22].

Measurements which can test these properties of QCD were recently performed in proton–lead ( $p+Pb$ ) collisions at the LHC [23, 24] and deuteron–gold ( $d+Au$ ) collisions at RHIC [25] at center of mass energies of 5.02 TeV and 200 GeV, respectively. In these data, the production of large transverse momentum ( $p_t$ ) jets was studied in the large- $x_p$  kinematic region as a function of hadronic activity in the downstream nucleus-going direction ( $\eta < -3$ ). Hadron production rates in this rapidity range are correlated with  $\nu$ , and have been experimentally shown to be insensitive to energy-momentum conservation effects related to jet production at mid- and forward (proton-going) rapidities [26] (though such correlations were expected in some models of the process under consideration [27]). Each experiment observed a qualitatively consistent picture: for events with jets originating from a large- $x_p$  scattering, the geometric (eikonal) model strongly underestimates the number of events with low hadronic activity (geometrically “peripheral” events in the classical picture) and overestimates those with a large hadronic activity (“central” events). However, inclusive jet production rates were unmodified,  $\sigma^{p+A} = A\sigma^{p+p}$ , as expected from QCD factorization and the small modification of the nuclear parton densities in this region [28].

In our previous analysis [2] we demonstrated that color fluctuation effects which led to a more weakly interacting large- $x_p$  configuration could quantitatively describe the ATLAS data for jet production at  $x_p \approx 0.6$ . In this paper, we present a unified analysis of ATLAS [23] and PHENIX [25] data to study the collision energy and  $x_p$ -dependence of this effect in detail. CMS has observed a qualitatively similar effect in the centrality dependence of di-jet production [24]. However, those data are pre-

sented with an open  $p_t$  selection and as a function of the system pseudorapidity  $(\eta_1 + \eta_2)/2$ , and thus integrate over a rather wide distribution of  $x_p$  values. Thus we do not include it in the present extraction, which relies on isolating narrow ranges of  $x_p$  values.

To model the effects of color fluctuations in  $p+A$  collisions, we use the Monte Carlo algorithm developed in Refs. [1, 29], of which we summarize the main features here. In our procedure, the probability distribution,  $P_N(\sigma)$ , for a projectile nucleon configuration to have a total cross-section for an interaction with another nucleon in the target,  $\sigma$ , is given by

$$P_N(\sigma) = C \frac{\sigma}{\sigma + \sigma_0} \exp \left\{ -\frac{(\sigma/\sigma_0 - 1)^2}{\Omega^2} \right\}. \quad (1)$$

Note here that configurations with small  $\sigma$  correspond to the color transparency regime which contributes very little to the phenomena we consider here.

The parameters of  $P_N$  are determined from analyses of data on diffractive processes in hadronic collisions, which are sensitive to the size of the fluctuations, as discussed in Ref. [30]. This form consistently accounts for several expected properties of the projectile hadron wave functions: (1) it follows from a generalization of the quark counting rules,  $P_N \rightarrow 0$  as  $\sigma \rightarrow 0$ ; (2)  $P_N$  is approximately Gaussian for  $\sigma \sim \sigma_0$ ; (3) the first two moments of the distribution give the conservation of probability ( $\int P_N d\sigma = 1$ ) and define the average total cross-section ( $\int P_N \sigma d\sigma = \sigma_{tot}$ ); (4) it smoothly interpolates between the expected behavior at small and large values of  $\sigma$  (the former of which is in the color transparency regime). A different parameterization of  $P_N$  at RHIC energies may be found in Ref. [31], and other approaches based on fluctuations in the positions of proton constituents are also discussed in the literature, see e.g. [32].

We determine the distribution of  $\nu$  values in  $p+A$  collisions by extending standard simulation procedures [33] to include fluctuations in the proton interaction strength and other effects. The spatial configuration of nucleons in the nucleus are generated according to a Woods-Saxon distribution but taking into account short-range  $NN$  spatial correlations which affect the nuclear two-body density [34]. The probability that the projectile nucleon interacts with a target nucleon varies with their transverse displacement according to the profile function of the interaction. In addition, the probability of a hard interaction was determined through the convolution of generalized parton distributions (which describe the longitudinal and transverse distributions of partons) in the projectile proton and target nucleons, as discussed in Ref. [1]. Thus, the model takes into account the spatial localization of hard partons close to the center of the nucleon [35].

One of the struck nucleons in the target is randomly chosen to contain the hard scattering, while the remain-

ing nucleons undergo soft interactions with the inelastic fraction of the fluctuating cross-section ( $\approx 0.75\sigma_{tot}$ ). For  $d+A$  collisions, the configuration of the deuteron is sampled according to the projection of its wavefunction into the transverse plane. In this way, the model provides the distribution over the number of  $NN$  interactions,  $\nu$ , for  $p/d+A$  collisions.

To explore how hard scattering rates are correlated with  $\nu$ , we define the ratio

$$\begin{aligned} R(\nu) &= (\sigma_\nu^{hard}/\sigma_\nu^{MB}) / (\nu \cdot \sigma_{NN}^{hard}/\sigma_{NN}^{MB}) \\ &= (\sigma_\nu^{hard}/\sigma_{NN}^{hard}) / (\nu \cdot \sigma_\nu^{MB}/\sigma_{NN}^{MB}), \end{aligned} \quad (2)$$

where  $\sigma_\nu^{hard}$  and  $\sigma_{NN}^{hard}$  are the hard process cross-section in  $p+A$  collisions with  $\nu$   $NN$  interactions and just in one  $NN$  collision, respectively, and  $\sigma_\nu^{MB}$  and  $\sigma_{NN}^{MB}$  are the analogues of these but for minimum bias (inelastic) collisions.  $R(\nu)$  is the ratio of the observed hard process rate to the rate expected given the number of (soft) inelastic  $NN$  interactions. Hence, the experiments observed  $R > 1$  for small  $\nu$ ,  $R < 1$  for large  $\nu$ , and  $R = 1$  for  $\nu$ -integrated collisions.

We define the  $x_p$ -dependent shrinking of the average interaction strength at a given collision energy  $\sqrt{s}$  as

$$\lambda(x_p) = \langle \sigma_{NN}^{MB}(x_p) \rangle / \sigma_{NN}^{MB}. \quad (3)$$

The distribution over the number of collisions is mainly sensitive to the value of  $\lambda(x_p)$ . It has a small sensitivity to the size of the fluctuations of  $\sigma_{NN}(x_p)$ . Hence, similar to what was done in Ref. [2], we model fluctuations in the strength of interaction at fixed  $x_p$  by assuming that the dispersion of  $\sigma$  at fixed  $x_p$  is similar to the average dispersion. As  $\lambda(x_p)$  decreases from unity, the deviations of  $R(\nu)$  from unity smoothly increase. For a given value of  $\lambda(x_p)$ , our model provides  $R(\nu)$  for each  $\nu$ .

The value of  $R(\nu)$  is schematically identical to the experimentally measured nuclear modification factors  $R_{pA}$  ( $R_{pPb}$  or  $R_{dAu}$ ), except that these are reported for different *centrality* selections: sets of events experimentally characterized by some range of hadronic activity at large nuclear-going rapidity. In  $p+Pb$  collisions in ATLAS [21], the hadronic activity is measured as the transverse energy sum,  $\Sigma E_T$ , in the hadronic calorimeter situated at  $-4.9 < \eta < -3.2$ , and is taken to be proportional to  $\nu+1$  (the total number of participating nucleons). In  $d+Au$  collisions in PHENIX [25], the hadronic activity is defined as the total charge measured in the beam-beam counter situated at  $-3.9 < \eta < -3.1$ , and is taken to be proportional to  $\nu$ . In both cases, the selected hadronic event activity (i.e. centrality) ranges result in sets of events with broad but well-separated distributions of  $\nu$ . To compare our model with the LHC and RHIC jet production data, we use the relationships between  $\nu$  and  $\Sigma E_T$  or charge

established by the experiments in Refs. [20, 21] to determine the distributions over  $\nu$  for each centrality selection. Thus, for each value of  $\lambda(x_p)$ , we calculate the nuclear modification factors,  $R_{pA}$ , weighted by the  $\nu$  distribution in each experimentally defined centrality selection.

Based on this model, we fit the ATLAS and PHENIX data in every bin of  $x_p \approx 2p_t \cosh(y)/\sqrt{s}$  reported in the experiments to find the best value of  $\lambda(x_p)$  which describes  $R_{pA}$  in all reported centrality selections. In both datasets, we compare to the so-called central-to-peripheral ratio,  $R_{CP}$ , which is the ratio of  $R_{pA}$  in a given central event selection to that in the most peripheral one. Since the centrality-averaged  $R_{pA}$  values are consistent with unity, the  $R_{CP}$  values encode the same information on the centrality dependence but with improved experimental uncertainties for our fits.

We determine the best  $\lambda(x_p)$  by minimizing the  $\chi^2$  summed over all centrality selections  $i$ ,  $\chi^2 = \sum_i (R_i^{data} - R_i^{model}(\lambda))^2 / \epsilon_i^2$  where  $\epsilon^2$  is taken to be the quadrature sum of the statistical and systematic uncertainties in the data. The RHIC and LHC data provide three and five centralities for each value of  $x_p$ , which are used to fit a single value of  $\lambda(x_p)$ , and they provide data on eight and ten values of  $x_p$  in total. In each  $x_p$  range, we estimate the uncertainty on the extracted value of  $\lambda(x_p)$  as the range over which the  $\chi^2$  increases by one.

We note that there may be additional uncertainties in the modeling of  $P(\sigma, s)$ , such as the variance of the distribution. These arise from the lack of appropriate diffractive  $pp$  data at RHIC and LHC energies, and are thus difficult to quantify. However, the reasonable agreement of the model with the data obtained at very different energies and kinematic selections below suggests that the observables considered here have only a moderate sensitivity to these details.

Figs. 2 and 3 show the full comparison of the predictions of our model to RHIC and LHC data, respectively.

Fig. 4 summarizes the results of our global analysis of  $\lambda(x_p)$  as a function of  $x_p$  and collision energy. In the case of the RHIC data, our analysis yields slightly smaller values of  $\lambda(x_p)$  than those in Ref. [36], due to differences in the treatment of the collision geometry. At low values of  $x_p \sim 0.1$ ,  $\lambda(x_p)$  is similar at both RHIC and LHC energies. At increasingly larger  $x_p$ ,  $\lambda(x_p)$  systematically decreases but does so faster at RHIC energies.

These findings verify our previous expectations in Ref. [2] and have a natural explanation. In perturbative QCD the total cross section for a bound state with a small transverse size  $\rho$  to interact with a nucleon is proportional to the gluon density  $g(Q^2, x_p)$  in the nucleon at resolution scales  $Q^2 \propto 1/\rho$  and  $x_p \sim Q^2/s$ . At large  $Q^2$ ,  $g$  grows quickly with decreasing  $x_p$ , resulting in an increase of the cross-section (and of  $\lambda(x_p)$  at fixed  $x_p$ ) for these small configurations with increasing collision energy. However, this increase is slower than what is observed for perturbative processes with vacuum exchange

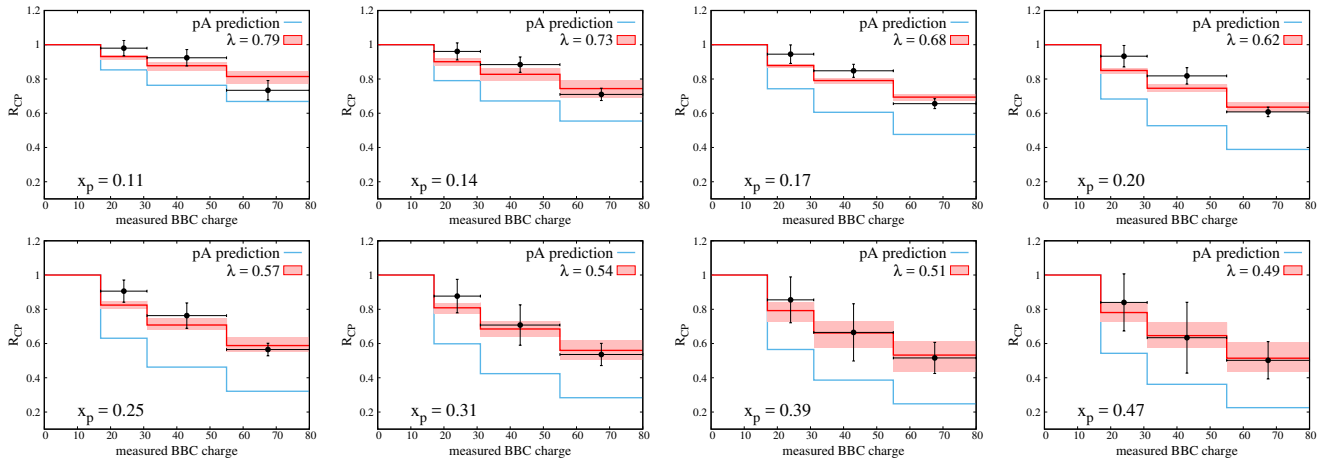


FIG. 2. Comparison of the RHIC deuteron–gold nuclear modification factor data (black points) in different hadronic activity bins, to those in our model (shaded band), and to predictions for proton–gold data at RHIC (blue line). Each panel shows a different  $x_p$  range.

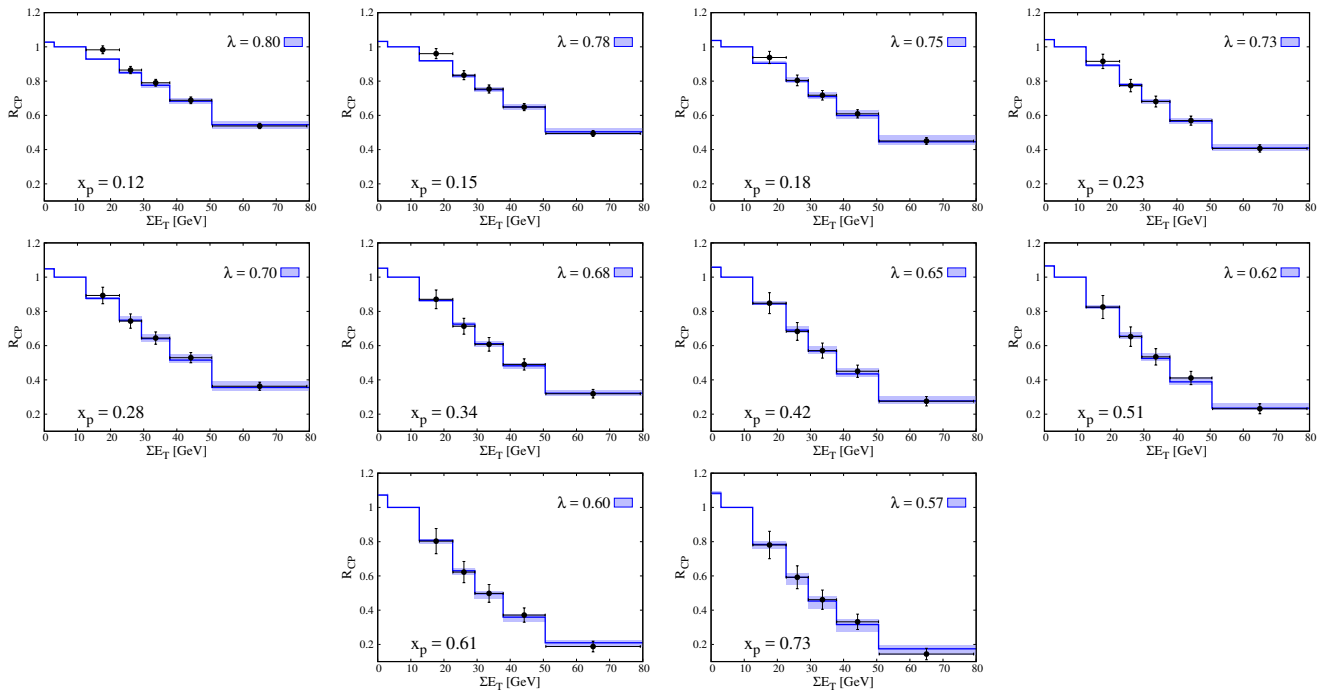


FIG. 3. Comparison of the LHC proton–lead nuclear modification factor data (black points) in different hadronic activity bins, to those in our model (shaded band). Each panel shows a different  $x_p$  range.

in t-channel, such as  $J/\psi$  exclusive photoproduction [15]. Thus the interaction at high energies may be thought of as lying between the perturbative and non-perturbative domains, suggesting that chiral symmetry is restored for the probed components of the light cone proton wave function. Finally, the fast growth of the cross section for small configurations is consistent with the expected narrowing of the  $P_N(\sigma)$  distribution at increasing collision energies [37].

A consistency check of our results can be performed

under the assumption that the probability to find a configuration with some large  $x_p$  is the same at two collision energies  $\sqrt{s_1}$  and  $\sqrt{s_2}$ . If the fluctuations in  $\sigma(x_p)$  are small such that, at fixed  $x_p$ , there is a one-to-one correspondence between  $\sigma(x_p)$  at two different energies, one may express this as the probability to find a configuration with cross section smaller than  $\lambda(x_p)\sigma_{tot}$ ,

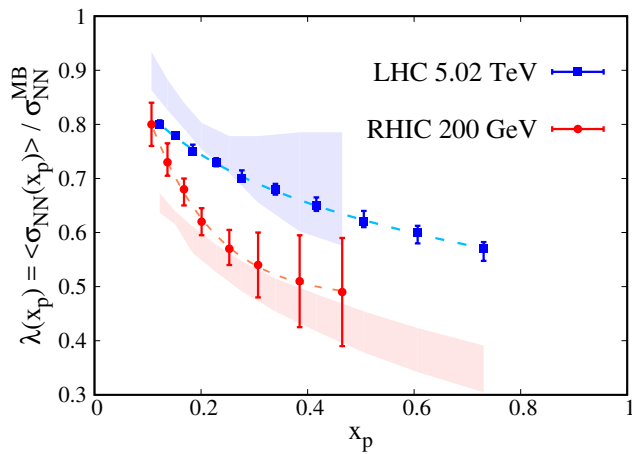


FIG. 4. Extracted values of  $\lambda(x_p)$  as a function of  $x_p$  at RHIC and LHC energies (solid points), with fits to an exponential function in  $x_p$  shown as dashed lines to guide the eye. The shaded bands are a prediction for  $\lambda(x_p)$  at each energy using the results at the other energy as input (see text).

$$\int_0^{\lambda(x_p; \sqrt{s_1}) \sigma_{tot}(\sqrt{s_1})} d\sigma P_N(\sigma; \sqrt{s_1}) = \int_0^{\lambda(x_p; \sqrt{s_2}) \sigma_{tot}(\sqrt{s_2})} d\sigma P_N(\sigma; \sqrt{s_2}), \quad (4)$$

which along with Eq. (1) is an implicit equation for the energy dependence of  $\lambda(x_p)$  at fixed  $x_p$ .

Starting with the LHC results for  $\lambda(x_p)$ , we use Eq. 4 to systematically predict  $\lambda(x_p)$  at RHIC energies at the same values of  $x_p$ , and vice versa. Fig. 4 shows the results of this check. For  $x_p \gtrsim 0.15$ , the relationship between the extracted  $\lambda(x_p)$  values at RHIC and LHC energies is consistent with that predicted by Eq. 4. At lower  $x_p$ , this method predicts a larger difference in  $\lambda(x_p)$  at the two energies than is extracted in data, suggesting that our model does not provide a complete description of color fluctuation phenomena in this  $x_p$  range (for example, since it ignores a possible parton flavor dependence). Using the parameterization for  $P_N(\sigma)$  at the lower, fixed-target energies given in Ref. [30], one finds that  $\lambda(x_p \sim 0.5) \approx 0.38$  at  $\sqrt{s} = 30$  GeV. At these lower energies, the large- $x_p$  quarks are thus localized in an area of transverse size  $\sqrt{\lambda(x_p)} \approx 0.6$  smaller than that in the average configuration, leading to them having a significantly larger nonperturbative transverse momentum.

Recently, data on 200 GeV proton-gold collisions were recorded at RHIC, allowing for a further test of our model. Using the same parameters which relate  $\nu$  to the hadronic activity as in the  $d$ +Au data, we calculate the distributions of  $\nu$  in example centrality bins and the  $R_{CP}$  values for hard triggers with different ranges of  $x_p$ . These predictions are summarized in Fig. 2. As also argued in Ref. [36], the magnitude of the observable effect should be larger than in the  $d$ +Au data, where it is expected to be washed out by the additional projectile nucleon.

The global analysis presented in this paper quantitatively extends our initial interpretation of the LHC data on forward jet production in  $p$ +A collisions as arising from an  $x_p$ -dependent decrease in the interaction strength of proton configurations [2], and demonstrates that the same picture successfully describes RHIC data on large- $x_p$  jet production. Our analysis finds that the suppression of the interaction strength is stronger at lower energies, consistent with expectations from QCD that cross-sections for small configurations grow faster with energy than do those for average configurations.

Measurements of other processes arising from a different mixture of large- $x_p$  quarks and gluons (e.g. Drell-Yan or electroweak processes) would allow for a comparison of quark- vs. gluon-dominated configurations. Analogous studies in ultraperipheral collision data [38] may probe color fluctuations in the photon wave function.

Our conclusions also have implications for understanding features in the quark-gluon structure of nuclei such as the observed suppression of the nuclear structure function at large- $x$ , commonly known as the EMC effect [39]. Since nucleons in a configuration with a large- $x$  parton are weakly interacting and the strength of the interaction at fixed  $x$  falls at lower energies, it is natural to expect that such configurations interact very weakly with other nucleons at the energy ranges relevant for nuclei. In the bound nucleon wavefunction, such weakly interacting nucleon configurations are strongly suppressed [14]. Thus, this picture suggests a natural explanation for the observed suppression of partons in the EMC effect region. This phenomenon may furthermore provide information on how the properties of nucleons experiencing large pressures may change, leading to, for example, the restoration of chiral symmetry within the core of neutron stars.

We thank B. Muller for the suggestion to present predictions for  $p$ +A running at RHIC within our framework, A. Mueller for discussion of proton squeezing at large  $x_p$ , and J. Nagle for suggestions on the manuscript. L.F.'s and M.S.'s research was supported by the US Department of Energy Office of Science, Office of Nuclear Physics under Award No. DE-FG02-93ER40771. D.V.P.'s research was supported by the US Department of Energy Office of Science, Office of Nuclear Physics under Award No. de-sc0018117.

- 
- [1] M. Alvioli and M. Strikman, "Color fluctuation effects in proton-nucleus collisions," Phys. Lett. **B722**, 347–354 (2013), arXiv:1301.0728 [hep-ph].
  - [2] M. Alvioli, B. A. Cole, L. Frankfurt, D. V. Perepelitsa, and M. Strikman, "Evidence for  $x$ -dependent proton color fluctuations in pA collisions at the CERN Large Hadron Collider," Phys. Rev. **C93**, 011902 (2016), arXiv:1409.7381 [hep-ph].
  - [3] I. Ya. Pomeranchuk and E. L. Feinberg, Dokl. Akad.

- Nauk SSSR **93**, 439 (1953).
- [4] E. L. Feinberg and I. Pomeranchuk, “High energy inelastic diffraction phenomena,” *Il Nuovo Cimento* **3**, 652–671 (1956).
- [5] L. Frankfurt and M. Strikman, “Diffractive phenomena in high energy processes,” in *100 Years of Subatomic Physics*, edited by Ernest M. Henley and Stephen D. Ellis (2013) pp. 363–423, arXiv:1304.4308 [hep-ph].
- [6] L. McLerran, “High Energy Nuclear Physics: From Bear Mountain to the LHC,” in *100 Years of Subatomic Physics*, edited by Ernest M. Henley and Stephen D. Ellis (2013) pp. 171–197.
- [7] M. Alvioli, G. Soyez, and D. N. Triantafyllopoulos, “Testing the Gaussian Approximation to the JIMWLK Equation,” *Phys. Rev.* **D87**, 014016 (2013), arXiv:1212.1656 [hep-ph].
- [8] L. L. Frankfurt, G. A. Miller, and M. Strikman, “The Geometrical color optics of coherent high-energy processes,” *Ann. Rev. Nucl. Part. Sci.* **44**, 501–560 (1994), arXiv:hep-ph/9407274 [hep-ph].
- [9] H. Heiselberg, G. Baym, B. Blaettel, L. L. Frankfurt, and M. Strikman, “Color transparency, color opacity, and fluctuations in nuclear collisions,” *Phys. Rev. Lett.* **67**, 2946–2949 (1991).
- [10] L. Frankfurt, G. A. Miller, and M. Strikman, “Coherent nuclear diffractive production of mini - jets: Illuminating color transparency,” *Phys. Lett.* **B304**, 1–7 (1993), arXiv:hep-ph/9305228 [hep-ph].
- [11] L. Frankfurt, G. A. Miller, and M. Strikman, “Coherent QCD phenomena in the coherent pion nucleon and pion nucleus production of two jets at high relative momenta,” *Phys. Rev.* **D65**, 094015 (2002), arXiv:hep-ph/0010297 [hep-ph].
- [12] E. M. Aitala *et al.* (E791), “Observation of color transparency in diffractive dissociation of pions,” *Phys. Rev. Lett.* **86**, 4773–4777 (2001), arXiv:hep-ex/0010044 [hep-ex].
- [13] The first theoretical study of the coherent dissociation of pions scattering off nuclei into two jets was performed in Ref. [40]. The obtained result contradicts the QCD factorization theorem [10, 11] and A-dependence and  $p_t$  dependence of the process measured in data [12].
- [14] L. L. Frankfurt and M. I. Strikman, “Point-like configurations in hadrons and nuclei and deep inelastic scattering reactions with leptons: EMC and EMC-like effects,” *Nucl. Phys.* **B250**, 143–176 (1985).
- [15] H. Abramowicz and A. Caldwell, “HERA collider physics,” *Rev. Mod. Phys.* **71**, 1275–1410 (1999), arXiv:hep-ex/9903037 [hep-ex].
- [16] S. J. Brodsky and G. R. Farrar, “Scaling Laws at Large Transverse Momentum,” *Phys. Rev. Lett.* **31**, 1153–1156 (1973).
- [17] S. J. Brodsky and G. R. Farrar, “Scaling Laws for Large Momentum Transfer Processes,” *Phys. Rev.* **D11**, 1309 (1975).
- [18] L. L. Frankfurt and M. I. Strikman, “High-Energy Phenomena, Short Range Nuclear Structure and QCD,” *Phys. Rept.* **76**, 215–347 (1981).
- [19] However, an opposite trend is present for the relativistic Gaussian wave function considered e.g. in [41]. For example, consider a meson with wave function  $\psi^2(x, k_t) \propto \exp(-c \cdot k_t^2 / (x(1-x)))$ . The transverse area occupied by a large  $x$  configuration grows as  $\propto 1/[x(1-x)]$ . At the same time, in the quark models which feature a singular short distance potential, such large- $x$  configurations do shrink.
- [20] A. Adare *et al.* (PHENIX), “Centrality categorization for  $R_{p(d)+A}$  in high-energy collisions,” *Phys. Rev.* **C90**, 034902 (2014), arXiv:1310.4793 [nucl-ex].
- [21] G. Aad *et al.* (ATLAS), “Measurement of the centrality dependence of the charged-particle pseudorapidity distribution in proton-lead collisions at  $\sqrt{s_{NN}} = 5.02$  TeV with the ATLAS detector,” *Eur. Phys. J.* **C76**, 199 (2016), arXiv:1508.00848 [hep-ex].
- [22] Jaroslav Adam *et al.* (ALICE), “Centrality dependence of particle production in p-Pb collisions at  $\sqrt{s_{NN}} = 5.02$  TeV,” *Phys. Rev.* **C91**, 064905 (2015), arXiv:1412.6828 [nucl-ex].
- [23] G. Aad *et al.* (ATLAS), “Centrality and rapidity dependence of inclusive jet production in  $\sqrt{s_{NN}} = 5.02$  TeV proton-lead collisions with the ATLAS detector,” *Phys. Lett.* **B748**, 392–413 (2015), arXiv:1412.4092 [hep-ex].
- [24] S. Chatrchyan *et al.* (CMS), “Studies of dijet transverse momentum balance and pseudorapidity distributions in pPb collisions at  $\sqrt{s_{NN}} = 5.02$  TeV,” *Eur. Phys. J.* **C74**, 2951 (2014), arXiv:1401.4433 [nucl-ex].
- [25] A. Adare *et al.* (PHENIX), “Centrality-dependent modification of jet-production rates in deuteron-gold collisions at  $\sqrt{s_{NN}} = 200$  GeV,” *Phys. Rev. Lett.* **116**, 122301 (2016), arXiv:1509.04657 [nucl-ex].
- [26] G. Aad *et al.* (ATLAS), “Measurement of the dependence of transverse energy production at large pseudorapidity on the hard-scattering kinematics of proton-proton collisions at  $\sqrt{s} = 2.76$  TeV with ATLAS,” *Phys. Lett.* **B756**, 10–28 (2016), arXiv:1512.00197 [hep-ex].
- [27] N. Armesto, D.C. Gülhan, and J.G. Milhano, “Kinematic bias on centrality selection of jet events in pPb collisions at the LHC,” *Phys. Lett.* **B747**, 441–445 (2015), arXiv:1502.02986 [hep-ph].
- [28] N. Armesto, H. Paukkunen, J. M. Penin, C. A. Salgado, and P. Zurita, “An analysis of the impact of LHC Run I proton-lead data on nuclear parton densities,” *Eur. Phys. J.* **C76**, 218 (2016), arXiv:1512.01528 [hep-ph].
- [29] M. Alvioli, L. Frankfurt, V. Guzey, and M. Strikman, “Revealing ”flickering” of the interaction strength in pA collisions at the CERN LHC,” *Phys. Rev.* **C90**, 034914 (2014), arXiv:1402.2868 [hep-ph].
- [30] B. Blaettel, G. Baym, L. L. Frankfurt, and M. Strikman, “How transparent are hadrons to pions?” *Phys. Rev. Lett.* **70**, 896–899 (1993).
- [31] C. E. Coleman-Smith and B. Müller, “Mapping the proton’s fluctuating size and shape,” *Phys. Rev.* **D89**, 025019 (2014), arXiv:1307.5911 [hep-ph].
- [32] Javier L. Albacete, Hannah Petersen, and Alba Soto-Ontoso, “Correlated wounded hot spots in proton-proton interactions,” *Phys. Rev.* **C95**, 064909 (2017), arXiv:1612.06274 [hep-ph].
- [33] C. Loizides, J. Nagle, and P. Steinberg, “Improved version of the PHOBOS Glauber Monte Carlo,” *SoftwareX* **1-2**, 13–18 (2015), arXiv:1408.2549 [nucl-ex].
- [34] M. Alvioli, H. J. Drescher, and M. Strikman, “A Monte Carlo generator of nucleon configurations in complex nuclei including Nucleon-Nucleon correlations,” *Phys. Lett.* **B680**, 225–230 (2009), arXiv:0905.2670 [nucl-th].
- [35] L. Frankfurt, M. Strikman, and C. Weiss, “Transverse nucleon structure and diagnostics of hard parton-parton processes at LHC,” *Phys. Rev.* **D83**, 054012 (2011), arXiv:1009.2559 [hep-ph].

- [36] D. McGlinchey, J. L. Nagle, and D. V. Perepelitsa, “Consequences of high- $x$  proton size fluctuations in small collision systems at  $\sqrt{s_{NN}} = 200\text{GeV}$ ,” *Phys. Rev.* **C94**, 024915 (2016), arXiv:1603.06607 [nucl-th].
- [37] V. Guzey and M. Strikman, “Proton-nucleus scattering and cross section fluctuations at RHIC and LHC,” *Phys. Lett.* **B633**, 245–252 (2006), [*Phys. Lett.*B663,456(2008)], arXiv:hep-ph/0505088 [hep-ph].
- [38] M. Alvioli, L. Frankfurt, V. Guzey, M. Strikman, and M. Zhalov, “Mapping color fluctuations in the photon in ultraperipheral heavy ion collisions at the Large Hadron Collider,” *Phys. Lett.* **B767**, 450–457 (2017), arXiv:1605.06606 [hep-ph].
- [39] O. Hen, G. A. Miller, E. Piassetzky, and L. B. Weinstein, “Nucleon-Nucleon Correlations, Short-lived Excitations, and the Quarks Within,” *Rev. Mod. Phys.* **89**, 045002 (2017), arXiv:1611.09748 [nucl-ex].
- [40] G. Bertsch, Stanley J. Brodsky, A. S. Goldhaber, and J. F. Gunion, “Diffractive Excitation in QCD,” *Phys. Rev. Lett.* **47**, 297 (1981).
- [41] Stanley J. Brodsky, “Hadron Spectroscopy and Dynamics from Light-Front Holography and Superconformal Algebra,” *Few Body Syst.* **59**, 83 (2018), arXiv:1802.08552 [hep-ph].